Blast effects of external explosions

Isabelle Sochet

Blast effects of external explosions

I. Sochet

Ecole Nationale Supérieure d'Ingénieurs de Bourges – Institut PRISME – UPRES EA 4229 – 88 bvd Lahitolle – 18020 Bourges cedex – France -

**Corresponding author:* isabelle.sochet@ensi-bourges.fr

Security considerations for industrial production and storage require characterization of the mechanical effects caused by blast waves resulting from a detonation or deflagration. This paper evaluates current analytical methods to determine the characteristic parameters of a blast wave with respect to the pressure, impulse and duration of the positive phase of the blast. In the case of a detonation, the trinitrotoluene (TNT) equivalent-based method determines the mass of TNT that is equivalent to the gas load used during the explosion and evaluates the characteristic parameters. A review of the energy values for TNT detonation is given, and the relationships used to calculate the TNT equivalent are proposed. The identification of the effects of the pressure wave following the explosion of a gaseous charge in free space equates the deflagration propagation to a piston. In the case of an explosion in an obstructed medium, the deflagration is considered to consist of a basic set of explosions involved in the generation of an intense blast wave. An explosion creates high pressures if the flame reaches high speeds, which occurs in the presence of turbulent flow at the source level or for a degree of confinement and obstruction in the medium.

Keywords: blast effects, detonation, deflagration, explosion, TNT, multi-energy method

1. Introduction

Explosions are associated with accidental releases of energy that produce large quantities of expanding gases. Indeed, most of the past incidents involving the explosion of gas clouds suggest that a fuel leak is a potential hazard. If a quantity of fuel is accidentally released into the atmosphere and mixes with air, then a cloud of flammable gas may result. If the cloud encounters an ignition source, then it may then develop into an intense blast or deflagration. However, the gas may have been initially stored as a compressed gas that was affected by a loss of containment. In all cases, a rapid expansion of gas leads to a blast or pressure wave that may have important consequences on the environment. Thus, the most important property of an explosion is the blast. The mechanical energy of the explosion creates a blast wave that moves rapidly in the surrounding air. The resulting pressure is caused by two contradictory phenomena: increasing pressure due to combustion and decreasing pressure due to gas expansion.

The shape of the blast wave is dependent on the type of explosion. Before the arrival of the blast

wave, the pressure in the system is at normal ambient pressure (P_0). For an ideal blast wave, the pressure increases instantaneously to a value of $P_0 + \Delta P_0$; it then slowly decreases to negative values, reaches a minimum and returns to ambient pressure. This type of blast wave, which is called a shock wave, is caused by a detonation. In the case of a deflagration, the pressure increase is slower and the maximum pressure is lower. In addition, the blast wave has a positive phase followed by a negative phase, or a "suction phase." Although damage is most often associated with the peak pressure, the duration and impulse of blast waves are also important parameters. A number of experiments conducted in recent years highlight the importance of confinement and obstacles as well as the influence of high flow speeds in the blast wave for the prediction of the characteristic parameters of an explosion, including the overpressure, impulse and duration of the positive phase.

To obtain an initial estimate of the characteristic parameters related to an explosion, simple methods are used, including the trinitrotoluene- (TNT) equivalent and multi-energy methods, which are appropriate for two different types of explosions. Of these two methods, the TNT-equivalent method is suitable for the analysis of detonations from solid charges or gas charges, whereas the multi-energy concept is useful in the study of gas charge deflagrations. Indeed, the explosion of TNT is characterized by a shock with a short duration in which a coupling between the shock wave and the flame front is observed. The multi-energy method better represents the underlying processes in the propagation of a flame front.

In this paper, an overview of simple methods is provided for the calculation of the pressure of blast waves resulting from detonations or the deflagration of gas loads.

2. Profiles of blast waves

The term "blast wave" is used to describe the shock wave that results from the detonation of an explosive charge. This name arises from the "strong wind" that accompanies the wave and is felt by a stationary observer as the wave passes. In addition, the term "shock wave" is generally used to describe a steep pressure gradient in which the wave pattern is not characterized in detail.

2.1. Detonations

In a detonation, a shock wave coupled to a flame front propagates through the reaction mixture at supersonic speeds relative to ambient gases. Therefore, for a given quantity of explosives, detonations are more destructive than deflagrations. Blast waves resulting from the detonation of strong explosives (e.g., TNT) exhibit close to ideal wave behavior due to the relatively small amount of explosives and the quick release of energy associated with a rapid chemical reaction. The pressure profile over time of an ideal blast wave can be characterized by its rise time, the peak overpressure, the duration of the positive phase and the total duration (Friedländer wave). In the most common case, by considering spherical explosions in air from chemical explosives, these quantities can be measured precisely in terms of the energy released, which is typically related to the mass of the explosive and is most commonly related to TNT. Thus, the change in pressure created by a detonation at a fixed distance R from the center of an explosion is shown in Figure 1.

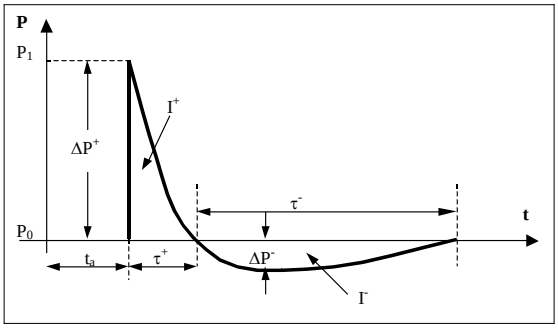

Fig. 1. Characteristic pressure profile of the blast wave resulting from a detonation

In this scheme, t_0 is the arrival time of the wave front, ΔP^+ is the positive pressure, t^+ is the duration of the positive phase, I^+ is the positive impulse, ΔP^- is the negative depression, t^- is the duration of the negative phase and I^- is the negative impulse. The impulse of the compression phase is calculated by using the following formula:

$$I^+ = \int_{t_a}^{t_a + \tau^+} \Delta P^+ \, dt$$

where the impulse of the rarefaction wave is given by:

$$I^- = \int_{t_a + \tau^+}^{t_a + \tau^+ + \tau^-} \Delta P^- \, dt$$

The duration of the compression wave and the rarefaction wave are important for analyzing the response of the target under the influence of the shock wave.
The time signal of the pressure wave can be represented with a Friedländer-type law

$$\Delta P(t) = \Delta P^+ . \left(1 - \frac{t}{t^+}\right) . e^{\frac{\alpha . t}{t^+}}$$

where ΔP^+ is the peak overpressure in the shock, and α is a dimensionless time constant, which depends on the incident pressure factor $\Delta P^+ / P_0$ relative to the ambient pressure P_0 as tabulated by Baker (1973).

Lannoy (1984) presented two types of profiles to describe the pressure wave if the blast wave is generated by the detonation of a gaseous charge, which includes a triangular model and a sinusoidal model.
The triangular shape is represented as:

$$\Delta P(t) = \Delta P^+ \times \left(1 - \frac{t}{t^+}\right) \times e^{\alpha t / t^+} \text{ if } 0 \le t \le \left(1 - \frac{\Delta P^-}{\Delta P^+}\right) \times t^+$$

$$\Delta P(t) = \Delta P^- \times \left(\frac{t - (t^+ + t^-)}{t^+ \times \left(1 - \frac{\Delta P^-}{\Delta P^+}\right) - (t^+ + t^-)} \right) \text{ if } \left(1 - \frac{\Delta P^-}{\Delta P^+}\right) \times t^+ \le t \le t^+ + t^-$$

This profile overestimates the positive impulse and underestimates the negative impulse.
The damped sinusoidal pressure wave profile is described by the following equation, where k is a constant:

$$\Delta P(t) = \Delta P^{+} \times \left(\frac{\sin\left(\frac{\pi}{t^{-}} . (t - t^{+}) \right)}{\sin\left(-\pi . \frac{t^{+}}{t^{-}} \right)} \right) \times \exp\left(-\frac{t}{k . t^{+}} \right)$$

This description yields better results in terms of the positive impulse and the negative impulse.
The damped sinusoidal wave models a profile that is more physically accurate and more precise for the positive impulse and the negative impulse, although the difference obtained for the total impulse is more important than in the case of the linear profile.
The damped sinusoidal profile was refined by Brossard et al. (1988) by the use of a coefficient k that was defined according to the reduced distance $\lambda = R / \sqrt[3]{E}$ and is within the validity range between 0.75 and 11.5 m.MJ$^{-1/3}$ and is expressed as:

$$\Delta P(t, \lambda) = \Delta P^{+} \times \left(\frac{\sin\left(\frac{\pi}{t^{-}} . (t - t^{+}) \right)}{\sin\left(-\pi . \frac{t^{+}}{t^{-}} \right)} \right) \times \exp\left(-\frac{k . t}{t^{+}} \right)$$

where $k = 0.811 - 0.055 \times \ln\lambda - 0.035 \times (\ln\lambda)^2$ for an incident wave.

The general shape of the pressure profile is similar for both charge gas detonations and solid explosives (TNT). However, the features described above are dependent upon the nature of the explosive charge. For example, two blast waves, one resulting from the detonation of a gas and one resulting from the detonation of TNT, may exhibit the same pressure amplitude but different impulse pressures and different positive phase durations (2003). The TNT explosion produces a more intense wave in the vicinity of the explosion and lower intensity shock waves at longer distances compared to a gas explosion in air for the same total amount of energy released. The explosion energy, the density of the energy released (energy linked to the volume of the charge) and the power (the rate of energy release) are parameters that determine the amplitude, duration and other characteristics of the blast wave. Four types of ideal sources of explosions include point sources, nuclear bombs, laser discharges and detonating explosives. Detonating explosives generate near-ideal waves due to their high density compared to air; therefore, the energy released per unit volume is significant. The blast wave is not maintained by the reactive medium from which it came, and its speed and its amplitude decrease with the distance traveled.

2.2. Deflagrations

In the case of a gas deflagration, the volume of a gas-air mixture is generally high and the energy release rate is relatively slow. This occurs because the chemical reaction is slower than in the case of a detonation. The blasts are characterized by more regular blast waves that propagate at a subsonic speed relative to the ambient gases. The flame propagation is initially associated with the conduction of heat and molecular diffusion. Initially, the flame propagation is laminar and the pressure effects are small. Then, as turbulence is generated, the combustion speed increases

and the pressure wave tends to become similar to an ideal wave. In the case of an explosion, negative pressures are important and cause damage as a result of the suction effect. The typical pressure profile induced by a blast over time at a given distance R is an "N" curve, which is shown in Figure 2 for the case in which the head wave is not a shock wave:

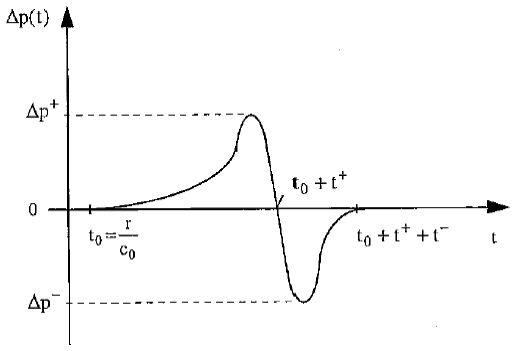

Fig. 2. Schematic profile of a typical pressure signal induced at a distance R by a deflagration

In contrast to a detonation, in the case of "slow" explosions, the depression phase has a negative maximum of the same order of magnitude as that in the maximum positive phase of the overpressure. The remaining environment returns to normal immediately after the arrest of the flame at a time $t = t_0 + t^+ + t^-$, where t^+ and t^- are the durations of the positive and negative phases of the ambient pressure, respectively. The positive and negative amplitudes of the pressure wave diminish with the distance 1/R, and the characteristic times t^+ and t^- are maintained for the entire field.

3. Thermodynamics of explosions – the case of TNT

The energy or heat released by the chemical reaction that occurs during the combustion of a propellant or detonation of an explosive is called the "heat of explosion" or "detonation heat". This value describes only the heat caused by the reaction of the explosive itself yielding the detonation products; therefore, this value does not include any heat generated by secondary reactions of the explosive or its products with air. Generally, the term "heat of explosion" is used for propellants, and the term "heat of detonation" is used for explosives. The combustion energy is a special case of reaction energy; it is the reaction energy required for the combustion of a reactant with a given amount of oxygen such that it is completely oxidized.
In an actual explosion, the composition of the products is not always the same for a given explosive. Factors such as the initial temperature and density, degree of confinement, particle size and morphology and the size and shape of the load affect the pressure and temperature behind the detonation front, where the products are rapidly expanding and a balance between the products is not achieved.

There is some confusion in the terminology related to the energy and heat of detonation, and the two are often used interchangeably. The heat of detonation is determined in a closed calorimetric tank and does not account for the energy available from the highly compressed gas products, which significantly contribute to the amount of energy transmitted to the blast wave, as outlined by Scilly (1995).
Thus, the term "detonation energy" will be used hereafter to refer to the calculated detonation energy of an explosive without the presence of air.

3.1. Oxygen balance

The detonation of an explosive is an oxidation reaction for which it can be assumed that all of the carbon forms CO_2, all of the hydrogen forms water and all of the nitrogen forms N_2. For the explosive composition $C_aH_bO_cN_dCl_eS_f$, the oxidation reaction is represented by:

$$C_aH_bO_cN_dCl_eS_f \rightarrow a\,CO_2 + 0.5(b-e)H_2O + 0.5\,d\,N_2 + e\,HCl + f\,SO_2 + \left[0.25(e-b) - (a+f) + 0.5\,c\right]O_2$$

The concentration of oxygen atoms in an oxidant is given by an oxygen balance (OB). This is an important term that indicates the oxidation potential and indicates the number of molecules of oxygen remaining after the oxidation of H, C, Mg, Al and so on to produce H_2O, CO_2, MgO_2 and so on. If the amount of oxygen in an explosive is limited and insufficient to obtain a complete oxidation reaction, then the amount of oxygen that is required to complete the reaction is preceded by a negative sign and the oxygen balance is negative. The oxygen balance is expressed as a percentage by mass:

$$OB = \frac{\left[0.25(e-b) - (a+f) + 0.5\,c\right] \times 32}{MW(\text{explosive})} \times 100\,(\%)$$

where MW (explosive) is the molecular mass of the explosive and is expressed in $g.mol^{-1}$. In conclusion, the oxygen balance (OB) provides information about the products: a positive value indicates an excess of oxygen in the explosive, whereas a negative value indicates that oxygen must be provided, typically by the surrounding air. If the oxygen balance is mostly negative, then there is not enough oxygen to form CO_2 and thus toxic gases such as CO will form. Regarding mixtures of explosives, detonation depends not only on the oxygen balance but also on combustion reactions and other physical properties.

The oxygen balance provides no information on the exchange of energy during the explosion. For 2,4,6-Trinitrotoluene (TNT), which has the chemical formula $C_7H_5N_3O_6$ and a molecular weight of 227 g mol^{-1}, the oxygen balance is mostly negative (-74%).

3.2. Decomposition rules

To clarify the problem related to the decomposition products (Akhavan, 2004), a set of rules was developed. The rules of decomposition are known as the Kistiakowsky-Wilson rules (KW rules), which are used for explosives in which oxygen deficits are moderate and the oxygen balance is higher than -40%, and are given as follows:

1 - The carbon atoms are converted into CO
2 - If oxygen remains, then hydrogen is oxidized to water
3 - If oxygen still remains, then CO is oxidized to CO_2
4 - All nitrogen is converted into N_2 gas

For explosives with an oxygen balance lower than -40%, the modified KW rules are used as follows:

1 - The hydrogen atoms are converted into water
2 - If oxygen remains, then the carbon is converted into CO
3 - If oxygen still remains, then CO is oxidized to CO_2
4 - All nitrogen is converted into N_2 gas

For TNT ($C_7H_5N_3O_6$), the products resulting from each rule are as follows:

- Rule 1: $5\,H \rightarrow 2.5\,H_2O$
- Rule 2: The remaining 3.5 atoms of oxygen $3.5\,O \rightarrow 3.5\,CO$
- Rule 3: There is no more oxygen
- Rule 4: $3\,N \rightarrow 1.5\,N_2$

The reaction of decomposition of TNT is:

$$C_7H_5N_3O_6 \rightarrow 3.5\,CO + 3.5\,C + 2.5\,H_2O + 1.5\,N_2$$

The Springall-Roberts rules (SR rules) are based the Kistiakowsky and Wilson rules and apply two additional conditions:

5 - One-third of CO formed is converted into carbon and CO_2

6 - A sixth of the original value of CO is converted with hydrogen to form C and water

The SR rules for TNT ($C_7H_5N_3O_6$) lead to the following decomposition:

- Rule 1: $6\,C \rightarrow 6\,CO$
- Rule 2: There are no more oxygen atoms
- Rule 3: There are no more oxygen atoms
- Rule 4: $3\,N \rightarrow 1.5\,N_2$

and the products are given as:

$C_7H_5N_3O_6 \qquad C_7H_5N_3O_6 \rightarrow 6\,CO + C + 2.5\,H_2 + 1.5N_2$

- Rule 5: 1/3 (6 CO) $= 2\,CO \rightarrow C + CO_2$

$$(6CO) + C + 2.5H_2 + 1.5N_2 \Rightarrow (4CO + C + CO_2) + C + 2.5H_2 + 1.5N_2$$

$$C_7H_5N_3O_6 \rightarrow 4\,CO + 2\,C + CO_2 + 2.5\,H_2 + 1.5\,N_2$$

- Rule 6: 1/6 (6 CO) $= 1CO$ and $1CO + H_2 \rightarrow C + H_2O$

and $(C + H_2O) + 3CO + 2C + CO_2 + 1.5H_2 + 1.5N_2$

Ultimately, the overall reaction is:

$$C_7H_5N_3O_6 \rightarrow 3C + 3CO + CO_2 + H_2O + 1.5\,H_2 + 1.5\,N_2$$

According to Scilly (1995), the decomposition equation recommended by Kamlet-Jacob (KJ rule) can be obtained from:

$$C_aH_bO_cN_d \rightarrow (a - 0.5\,c + 0.25\,b)\,C + (0.5\,c - 0.25\,b)\,CO_2 + (0.5\,b)\,H_2O + (0.5\,d)\,N_2$$

In this scheme, CO is not preferentially formed, and CO_2 is assumed to form as the only oxidation product of carbon and water and always forms at the beginning of the reaction. For TNT, the decomposition is then:

$$C_7H_5N_3O_6 \rightarrow 5.25\,C + 1.75\,CO_2 + 2.5\,H_2O + 1.5\,N_2$$

Kinney (1985) considered that all of the oxygen is contained in the carbon monoxide, which implies, in the case of TNT, the following chemical equation:

$$C_7H_5N_3O_6 \rightarrow C + 6\,CO + 2.5\,H_2 + 1.5\,N_2$$

3.3. Detonation energy

3.3.1. Literature review

Tongchang et al. (1995) performed experiments using a blast calorimeter in which the bomb had a cylindrical internal volume of 5 L and could support a pressure of 200 MPa. The experiments were performed with maximum loads of 50 g. The explosive force was measured according to the nature of the cartridge (porcelain, brass) and its thickness. All of the tests resulted in values between -4.31 and -4.40 $MJ.kg^{-1}$. These values are in agreement with the values used by Gelfand (2004), -4.517 $MJ.kg^{-1}$, Baker (1973), -4.520 $MJ.kg^{-1}$, Pförtner (1977), -4.686 $MJ.kg^{-1}$, de Lannoy (1984), -4.690 $MJ.kg^{-1}$ and the average from of the two energies in the work of Trelat (2006), who cited an energy of explosion of -4.600 $MJ.kg^{-1}$. Other values for the explosive force are cited by Filler (1956) including the calculated energy in the Encyclopedia of Chemical Technology, -3.87 $MJ.kg^{-1}$, the results of Tonegutti using a 2 g charge with a conventional calorimeter (detonation energy of -3.210 $MJ.kg^{-1}$) and, for a load of 100 g, the energy measured by the Armaments Research Establishment using calorimetry (-4.535 $MJ.kg^{-1}$). Omanga et al. (2009) used an energy value of -4.260 $MJ.kg^{-1}$ to characterize the propagation of shock waves following the detonation of spherical and hemispherical loads of 1 kg of TNT. Thus, all of the energies of detonation reported here range from a minimum of -3.21 $MJ.kg^{-1}$ (Filler, 1956) to a maximum of -4.832 $MJ.kg^{-1}$ (Cooper, 1996). These values have an average value of -4.369 $MJ.kg^{-1}$.

3.3.2. Helmholtz free energy method

The detonation energy corresponds to the explosive energy transmitted from the shock wave and the associated wind, i.e., the work done in the expansion of gases produced during the explosion, and is given by $\int_{initial}^{final} P.\Delta V$. By applying the first and second laws of thermodynamics, the change in the Helmholtz free energy can be used to calculate the energy of the explosion expressed in terms of the internal energy ΔU and entropy ΔS:

$\Delta F = \Delta U - T.\Delta S$ with $\Delta U = \Delta H - R.T.\Delta n$

and $\Delta H = \Delta H_p - \Delta H_r$; $\Delta n = n_p - n_r$; $\Delta S = \Delta S_p - \Delta S_r$

The index "p" represents the products while "r" represents the reagents.

3.3.3. Enthalpy method

The reaction energy is the energy released by the reaction, which is calculated by the enthalpy change involved in the chemical reaction between the standard state reaction products and the reagents.

3.3.4. Application to TNT

In this study, a comparative study of the energy values of detonation is proposed. The thermochemical data (enthalpy and entropy) are reported in Tables 2.4-2.6 and are compared among several sources.

Table 1
Data for the enthalpies of the detonation products

Enthalpy H (kJ.mol^{-1})	ASTM (2001)	NASA	Cooper (1996)	Kinney (1985)	Meyer (1987)
CO	-110.541	-110.541	-110.523	-118.8	-110.6
CO_2	-393.296	-393.505	-393.512		-303.8
H_2O (gas)	-241.8352	-241.835	-241.826		-303.8
H_2O (liquid)			-285.840		-286.1

Table 2
Data for the entropies of the detonation products

Entropy S (J.mol^{-1}.K^{-1})	ASTM (2001)	NASA	Kinney (1985)
C	5.74	5.686	5.700
CO	197.527	197.652	197.500
CO_2	213.886	213.802	213.700
H_2O (gas)	172.213	188.824	188.700
H_2O (liquid)			69.900
H_2	130.678	130.666	130.700
N_2	191.606	191.460	191.500

Table 3
Formation enthalpy and entropy of 2,4,6-Trinitrotoluene (TNT)

TNT - H (kJ.mol^{-1})	-26.00 (Van den Berg, 1985) ; -41.13 (Harrison, 1987); -54.40 (Kinney, 1985); -54.49 (Naz); -59.47 (Meyer, 1987)
TNT - S (J.mol^{-1}.K^{-1})	272.00 (Kinney, 1985); 271.96 (Naz); 554.00 (Harrison, 1987)

In those studies, the detonation energy was calculated, according to the authors, by considering water to be either in the vapor phase or the liquid phase. To study the influence of the physical state of water in this study, the calculations were performed systematically by considering the two different states. The thermodynamic data used in the calculations were from NASA, with the exception of the enthalpy and entropy of liquid water for which the values from Cooper (1996) and Kinney (1985) were used, respectively. The influence of the value of the enthalpy of the explosive was also studied (Tables 4-9)

Table 4
Detonation energies calculated for different decomposition patterns
- Enthalpy of TNT: ASTM (2001)

E detonation (MJ.kg^{-1})	Kistiakowsky et Wilson	Springall et Roberts	Kamlet et Jacob	Kinney
Free energy – H_2O gas	– 5.867	– 5.792	– 6.792	– 4.861
Enthalpy – H_2O gas	– 4.185	– 4.077	–5.514	– 2.739
Free energy – H_2O liquid	– 5.961	– 5.829	– 6.886	– 4.861
Enthalpy – H_2O liquid	– 4.669	– 4.271	– 5.998	– 2.739

Table 5
Detonation energies calculated for various decomposition patterns
- Enthalpy of TNT: NASA

E detonation ($MJ.kg^{-1}$)	Kistiakowsky et Wilson	Springall et Roberts	Kamlet et Jacob	Kinney
Free energy – H_2O gas	– 4.018	–5.733	– 6.734	– 4.747
Enthalpy – H_2O gas	–4.126	– 4.018	– 5.455	– 2.626
Free energy – H_2O liquid	– 5.903	– 5.771	– 6.828	– 4.802
Enthalpy – H_2O liquid	– 4.611	– 4.212	– 5.939	– 2.681

Table 6
Detonation energies calculated for various decomposition patterns
- Enthalpy of TNT: Cooper (1996)

E detonation ($MJ.kg^{-1}$)	Kistiakowsky et Wilson	Springall et Roberts	Kamlet et Jacob	Kinney
Free energy – H_2O gas	– 5.753	– 5.678	– 6.678	– 4.747
Enthalpy – H_2O gas	– 4.071	– 3.963	–5.399	– 2.626
Free energy – H_2O liquid	– 5.848	– 5.716	– 6.773	– 4.747
Enthalpy – H_2O liquid	– 4.556	– 4.157	–5.884	–2.626

Table 7
Detonation energies calculated for various decomposition patterns
- Enthalpy of TNT: Kinney (1985)

E detonation ($MJ.kg^{-1}$)	Kistiakowsky et Wilson	Springall et Roberts	Kamlet et Jacob	Kinney
Free energy – H_2O gas	– 5.808	– 5.733	– 6.734	– 4.802
Enthalpy – H_2O gas	– 4.126	– 4.018	– 5.455	– 2.681
Free energy – H_2O liquid	– 5.903	– 5.771	– 6.828	– 4.802
Enthalpy – H_2O liquid	– 4.6107	– 4.212	– 5 939	– 2.681

Table 8
Detonation energies calculated for various decomposition patterns
- Enthalpy of TNT: Akhavan (2004)

E detonation ($MJ.kg^{-1}$)	Kistiakowsky et Wilson	Springall et Roberts	Kamlet et Jacob	Kinney
Free energy – H_2O gas	– 5.934	– 5.858	– 6.858	– 4.927
Enthalpy – H_2O gas	– 4.251	– 4.143	– 5.580	– 2.806
Free energy – H_2O liquid	– 6.028	– 5.896	– 6.953	– 4.927
Enthalpy – H_2O liquid	– 4.736	– 4.337	– 6.064	– 2.806

Table 9
Detonation energies calculated for various decomposition patterns
-Enthalpy of TNT: Meyer (1987)

E detonation ($MJ.kg^{-1}$)	Kistiakowsky et Wilson	Springall et Roberts	Kamlet et Jacob	Kinney
Free energy – H_2O gas	– 5.786	– 5.711	– 6.711	– 4.780
Enthalpy – H_2O gas	– 4.104	–3.996	–5.433	– 2.659
Free energy – H_2O liquid	– 5.881	– 5.749	– 6.805	– 4.780
Enthalpy – H_2O liquid	– 4.588	–4.189	– 5.917	–2.659

This analysis indicates that the detonation energy calculated using the enthalpy method with the Kinney model (1985) resulted in values between -2.6 and -2.8 $MJ.kg^{-1}$, which are far below previously measured values; these values are also independent of the state of water due to its absence in the burned gases. However, the Helmholtz free energy calculated with this same pattern results in a value approximately 1.8 times greater, which is in agreement with the energy values that were determined experimentally and reported in the literature. The decomposition scheme proposed by Kamlet and Jacob consistently yielded much higher detonation energies regardless of the calculation method used. In the case of other patterns of decomposition, the detonation energies calculated using the Helmholtz free energy method are above the average values and are in the range of -5.7 and -5.9 $MJ.kg^{-1}$.
If the water is in liquid form, then the energies of detonation are higher than those obtained if the water is in vapor form, and these values more closely approximate the average value in the literature.
All of the calculations are in agreement with the study by Scilly (1995) in which the two physical states of water and several decompositions were considered. Overall, the value of the enthalpy of formation for explosive 2,4,6-Trinitrotoluene (TNT) has only a small influence.
It is important to determine which value should be used from all of the data and calculations presented above. From these data, it is possible to continue using the patterns of decomposition described by Kistiakowsky and Wilson or Springall and Roberts, which are applied if the water is in the liquid state. The detonation energy that was calculated on the base of enthalpy method and using the Kistiakowsky and Wilson rules with thermochemical data from Akhavan (2004) resulted in a value (-4.34 $MJ.kg^{-1}$) that was closest to the average value (-4.4 $MJ.kg^{-1}$) defined in the literature.

4. TNT equivalent

4.1. Overview

Generally, the TNT equivalent represents the mass of TNT that would result in an explosion of the same energy level as the unit weight of the explosive under consideration. Specifically, the TNT equivalent is defined as the ratio of the mass of TNT to the mass of the explosive that results in the same magnitude of blast wave (or impulse pressure) at the same radial distance for each charge, which assumes the scaling laws of Sachs and Hopkinson. All explosives generate blast waves that exhibit similar characteristics. The primary reason for choosing TNT as an explosive reference is that there is a large amount of experimental data regarding the characteristics of blast waves associated with this explosive. There are several methods for determining the explosive characteristics of different explosives, but they do not yield the same

values for the TNT equivalent. These values depend on the characteristic parameter of the blast wave, the geometry of the load and the distance from the explosive charge. The mechanism of energy release during the detonation process varies depending on the nature of the explosive. Explosives are generally composed of two parts: an oxidizer and a fuel. Pure explosives, which are called "ideal" explosives, have a threshold of molecules for each component defined for different mixtures of explosives. Due to the effects of the shock wave during detonation, the oxidizer and fuel interact in the area near the chemical reactions. The speed of the chemical reaction and the detonation velocity for ideal explosives are greater because more favorable conditions result in a greater efficiency. However, a larger detonation velocity results in a higher rate of energy release. Furthermore, the amount of energy released is directly proportional to the overpressure and the impulse of the blast wave. The reaction between gaseous products due to degradation of the explosive for a non-ideal explosive occurs beyond the chemical reaction zone, and the energy released after the reaction cannot withstand the blast wave.
In summary, an overview of different approaches for the determination of a TNT equivalent is given. It is possible to distinguish between approaches based on the pressure, impulse, Chapman-Jouguet state, explosion yield and the conventional methods of the Health and Safety Executive.

4.2. Pressure-based concept

Esparza (1986) based the equivalence of the incident pressure as the mass ratio of TNT to the considered explosives that cause the peak pressure at the same radial distance of each load. The equivalent mass of an explosive pressure is then:

$$E_P - TNT = \frac{M_{TNT}}{M} = \left(\frac{Z}{Z_{TNT}} \right)_{P\,cst}^3$$

where Z is the reduced distance.

Ohashi et al. (2002) and Kleine et al. (2003) described a procedure to calculate the TNT equivalent. This approach is based on knowledge of the shock radius - time of arrival diagram of the shock wave for the explosive under consideration. These data are used to calculate the Mach number of the shock and the peak overpressure as a function of distance (Dewey, 2005). The TNT equivalent pressure is between 0.4 and 0.6 for a stoechiometric propane-oxygen charge of 19281 kg.

4.3. *Impulse-based concept*

A similar approach is used to obtain the equivalent mass of impulse (Esparza, 1986):

$$E_I - TNT = \frac{M_{TNT}}{M} = \left(\frac{Z}{Z_{TNT}} \right)_{I\,cst}^3$$

However, the impulses are reported as the cube root of the mass, and the equivalent impulse is obtained by moving the curves along the diagonal.

4.4. Chapman-Jouguet state-based concept

Cooper (1996) defined the energy equivalent of TNT from the hydrodynamics of the Chapman-Jouguet (CJ) detonation state:

$$E_{CJ} - TNT = \frac{P_{CJ} / (2\ \rho_{CJ})}{P_{CJ\ TNT} / (2\ \rho_{CJ\ TNT})}$$

where $P_{CJ} = \frac{\rho_0 D_{CJ}^2}{4}$, $\rho_{CJ} = \frac{4\rho_0}{3}$ and $\frac{P_{CJ}}{2\ \rho_{CJ}} = \frac{3D_{CJ}^2}{32}$

Thus, the equivalent energy of TNT for a given explosive is expressed as:

$$E_{CJ} - TNT = \frac{D_{CJ}^2}{D_{CJ\ TNT}^2}$$

Jeremie et al. (2006) expressed the dependence of pressure P_{CJ} and detonation velocity D_{CJ} on the mass energy E of detonation:

$P_{CJ} = 2\left(\gamma_{CJ} - 1\right)\rho_0 E$ and $D_{CJ} = \sqrt{2\left(\gamma_{CJ}^2 - 1\right)E}$

where γ_{CJ} is the adiabatic constant of the detonation products, and ρ_0 is the density of the explosive.

4.5. Explosion yield-based concept

Lannoy (1984) conducted an anlysis of 150 incidents that resulted in accidents and fires in the gas, oil and chemical industries. The results are representative of 23 accidents for which the data are sufficient to yield a calculation of the explosion.

The database relies on the same pressure-based approach. The TNT equivalent of an explosive or explosive gas mixture is the mass of TNT that causes an explosion with the same pressure field as one kilogram of the explosive.

The energy equivalence is defined by the following ratio:

The upper limit of this ratio is:

$$\frac{\text{Heat of combustion of the hydrocarbon}}{\text{Calorific power of TNT}} \text{ where } \frac{46900\ \text{kJ.kg}^{-1}}{4690\ \text{kJ.kg}^{-1}}$$

Thus, we can define the theoretical equivalence energy as 10 kg of TNT for 1 kg of hydrocarbon; however, the validity of this value should be determined. To determine the validity, Lannoy (1984) suggested a total return of explosion η_e to establish a comparison with the analysis of the 23 accidents. The explosion yield is defined by the ratio:

$$\frac{\text{TNT mass equivalent energy of combustion}}{\text{Energy of combustion of the liberated product mass}}$$

considering:

$$E - TNT = \frac{\text{Mass of the TNT equivalent x } 4690\ \text{kJ.kg}^{-1}}{\text{Mass of the released product x Q kJ.kg}^{-1}}$$

In these equations, Q is the energy released by the complete combustion in air of a unit mass of the product under consideration.

Table 10
Severity of explosions (Lannoy, 1984)

Range Performance (%)	Representative Value (%)	Empirical equivalence kg TNT per kg flammable hydrocarbon	Corresponding frequency	Cumulative frequency
$0 \le E - TNT \le 6$	4	2	0.80	0.80
$6 \le E - TNT \le 12$	10	5	0.17	0.97
$12 \le E - TNT \le 18$	16	8	0.03	1.00

Table 10 shows a severity scale for explosions. If an accidental explosion occurs, then the resulting damage can be determined by using a TNT equivalence of 2 for a mass of hydrocarbon within the flammability limits. The resulting damage accounts for 80% of all of the possible damage. The strongest effects are observed for a TNT equivalent of 8 and the probability of observing such a system during actual explosions is greater than 3%.

Thus, the validity of the theoretical energy equivalence can be determined. A value of 10% should be used in a safety analysis to estimate the pressure effects because this value corresponds to a confidence level of 97%. An explosion yield of 10% corresponds to a 5 kg TNT equivalent of 1 kg of hydrocarbon in the atmosphere.

4.6. Conventional TNT equivalent method from the Health and Safety Executive (1986)

The conventional TNT equivalent method recommended by the Health and Safety Executive (HSE) applies to the case of liquid fuel spilled on the ground of the environment. The mass of the TNT equivalent charge is related to the total quantity of fuel in the cloud, which is determined by the following procedure:

• 1st stage: determination of the fraction of fuel F

The fraction F of liquid fuel released is calculated by using the following equation:

$$F = 1 - \exp\left(-\frac{c_p \, \Delta T}{L_v} \right)$$

where c_p is the mean specific heat ($kJ.kg^{-1}.K^{-1}$), ΔT is the temperature difference between vessel temperature and the boiling temperature at ambient pressure, and L_v is the latent heat of vaporization.

• Step 2: mass of fuel w_f in the cloud

The mass of fuel in the cloud is equal to the fraction of fuel multiplied by the quantity of fuel released. To report the charge in free-air without ground effects, a factor of 2 is applied as

$w_f = 2 F m_f$, where m_f is the total quantity of fuel released

• Step 3: mass of the charge of TNT equivalent

$$w_{TNT} = \eta_e \frac{w_f \, H_f}{H_{TNT}}$$

where w_{TNT} is the mass equivalent of TNT (kg), w_f is the mass of fuel in the cloud (kg), H_f is the heat of combustion of the fuel ($MJ.kg^{-1}$), H_{TNT} is the detonation energy of TNT (4.68 $MJ.\ kg^{-1}$) and η_e is the efficiency factor for TNT $(\eta_e = 0.03)$.

• Step 4: overpressure blast wave

If the equivalent mass of TNT is known, then the overpressure of the blast wave following the detonation of the charge gas can be determined. The peak overpressure produced by the detonation of the TNT charge is plotted against the scale of distance $\overline{R}$ from the load.

$$\overline{R} = \frac{R}{W_{TNT}^{1/3}}$$

where $\overline{R}$ is the Hopkinson reduced distance ($m.kg^{-1/3}$), w_{TNT} is the mass equivalent of TNT (kg) and R the actual distance of the load (m).

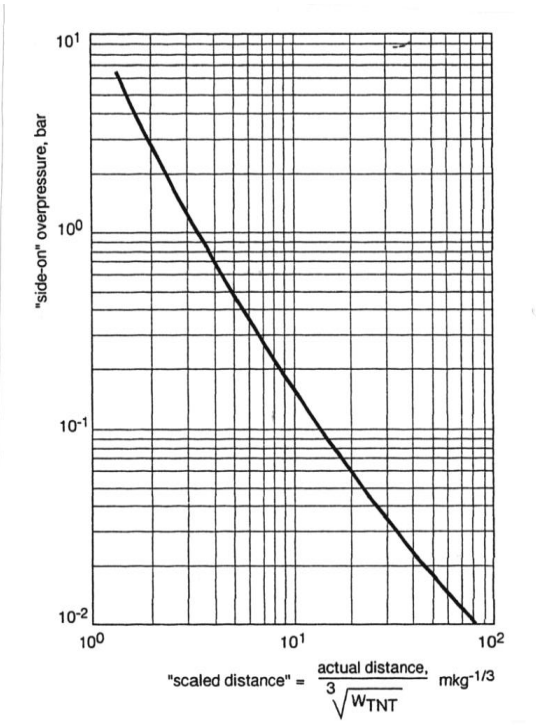

Fig. 3. Overpressure as a function of reduced distance (CPR, 1997)

4.7. A universal TNT equivalent

A universal TNT equivalent can be developed with respect to the charges of gas or other explosives. The complexity of combustion, the initial conditions and the geometry of the charge constructing the TNT equivalent depend not only on the nature of the explosive charge but also on the parameter of interest (pressure, impulse, duration of positive phase) and its distance from the center of the explosion.

In previous study (Sochet et al. ,2008), a dimensionless characteristic parameter of the blast wave was proposed, and an analysis of equivalent TNT charge gas was conducted as follows:

- Kogarko et al. (1966) stoichiometric C_3H_8-air mixtures, spherical volume of 10-15 m^3.
- Brossard et al. (1985) stoichiometric C_2H_2-air mixtures, C_3H_8-air, C_2H_4-air spherical volumes (placed at a height without ground effects) and hemispheres ranging from 1.6 to 510 m^3.
- Dorofeev et al. (1995a,b) stoichiometric and rich mixtures of C_3H_8-air hemispheres with volumes of 134 m^3.
- Dewey (2005) stoichiometric C_3H_8-air mixtures, spherical volume equivalent to 14,479 m^3.
- Behrens et al. (1975) ethylene-air mixtures (poor, rich and stoichiometric), hemispherical volumes from 0.72 to 7.54 m^3.
- Trélat et al. (2007) laboratory scale tests, stoichiometric C_3H_8-O_2 mixtures, hemispherical volumes of $7x10^{-4}$ m^3.

This dimensionless parameter allows for a consideration of the environmental conditions at the time of the explosion.

The equivalent TNT pressures confirm the variation with distance. All of the results exhibit a wide dispersion because the energy yields range from 0.5 to 0.9. However, the equivalent TNT impulse can be considered to be nearly constant and close to a mean value of 0.5.

4.8. Limitations of the TNT equivalent method

All of the methods used to determine the TNT equivalent are based on the fact that a potential explosion of a large cloud of gas is proportional to the total amount of fuel present in the cloud, whether or not it is within flammable limits. The power of the explosion of a gas cloud is expressed as a charge of equivalent TNT energy. The factor of proportionality is determined from the damage observed in a large number of incidents of exploding gas clouds. By accounting for the equation for the detonation products, the effects of detonation are influenced by basic parameters such as detonation celerity, pressure, energy detonation and the number of moles of the detonating gas. These values can be obtained from thermochemical calculations, and an average value can be obtained.

$$E-TNT = k_1 \frac{n_{HE}}{n_{TNT}} + k_2 \frac{E_{HE}}{E_{TNT}} + k_3 \frac{P_{HE}}{P_{TNT}} + k_4 \frac{D_{HE}}{D_{TNT}}$$

where k_1, k_2, k_3 and k_4 are empirical coefficients that were obtained experimentally (Jeremie et al., 2006).

Regarding the various methods, Gelfand (2004) proposed to define a mean value. This mean value defines the TNT equivalent energy by using the ratio of the detonation energy of an explosive to the detonation energy of TNT. However, the determination of the exact value of the detonation energy is difficult, and its value ranges from -2.673 to -6.702 $MJ.kg^{-1}$ based on the rule of decomposition and the thermodynamic data that were selected. This implies that the TNT equivalent values can be affected by a factor of 0.15 to 0.37.

The TM5-1300 diagrams (1969) are based on experiments with condensed explosives, but the blast wave produced by a gas explosion does not exhibit the same shape. Indeed, for a given peak overpressure, a blast wave resulting from the detonation of a gaseous charge has a positive phase duration and thus greater impulse.

In practice, the calculation of the TNT equivalent can evaluate the effects of an explosion. However, the abacus were constructed for ideal blast waves, point sources and for explosions that occur in free air, whereas industrial facilities contain more complex configurations with non-ideal explosions. The TNT equivalent method is based on the approximation of a point source for an explosion in which the energy is released from a cloud and is not homogeneous or three-dimensional. The isopressures are considered to be spherically symmetric from the point source and are assumed to be at the origin of the blast wave; therefore, there is no relationship to the geometry of the cloud. To the knowledge of the authors, only Lannoy (1984) proposed an approach to account for the non-spherical shape of the curves of isodamage; he considered the minimum and maximum distance for which the same damage was observed that was associated with the minimum and maximum explosive yields. The non-spherical shape of the isodamage curve may be due to the geometry of the site where the explosion occurred, the effect of wind in the case of a gas release and the formation of a gas cloud before initiation. Despite these drawbacks, the TNT equivalent method for the determination of the blast resulting from the detonation of explosive is the simplest method.

5. Blast waves resulting from an explosion in free space

If a diverging spherical flame front, which is centered on a point, propagates in a fuel charge with a characteristic spatial speed D, then the ambient gases located upstream of the flame front

are forced to move. This motion is effectively caused by a volume expansion of the ambient gases converting into burning gases.

In cases where the gases are assumed to be ideal and the propagation regime is stationary (i.e., the structure of the spherical laminar flame front and the fundamental speed of the flame does not change) and the reference frame is related to the gas flow then the speed D of the flame front relative to the ambient gas is proportional to the fundamental speed V_F and is expressed by $D=\alpha^{-1}V_F$, where $\alpha=\rho_b/\rho_f$ is the volume expansion ratio of the fuel mixture. The speed of the ambient gas immediately before the shock is defined as: $u_f=D(1-\alpha)$.

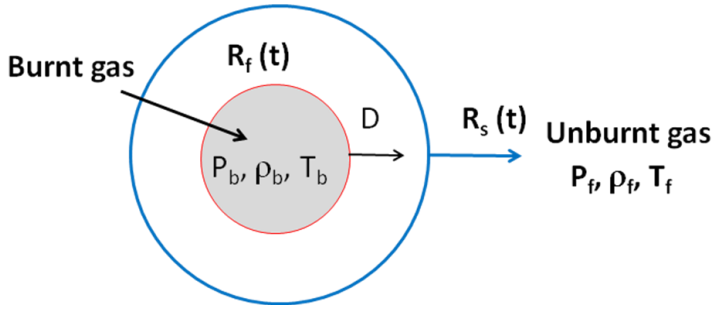

Fig. 4. Propagation of explosion deflagration in an open field

At time t, the flame front is located at $R=R_F$ and moves at a speed of D (Fig. 4). In the equation $R=R_s$, the wave head moves the ambient gas that was previously at rest. Physically, the deflagration affects the surrounding environment as a semi-permeable spherical piston for which the spatial velocity is directly dependent on the speed D of the flame and the expansion ratio α of the density of the ambient gas ρ_b. The speed of the blast depends on the characteristics of the ambient gas flow that lies in the propagation, and it is necessary to identify the velocity field and pressure of the ambient gas to obtain the velocity of the flame front in the fuel charge.

The piston model is the primary method for determining the characteristics of the pressure wave following the gas deflagration in free air. Solutions based on a modification of the Sachs method are also proposed.

5.1. Piston model

This model was developed by Deshaies et al. (1981) to relate, in the case of a spherical divergent deflagration, the pressure induced in the space at a distance Rto the propagation of the flame radius $R_f(t)$ at each moment. In this model, the flow generated by the flame is identical to that produced by a semipermeable spherical piston P moving (from R = 0 and at time t = 0) at a speed of u_p, which is directly related to the speed D of the deflagration.

5.1.1. Deflagrations at constant speeds

Here, D is considered to be constant, and thus the piston speed is constant and the two velocities are related by:

$$u_p=D(1-\alpha)$$

The complete analytical solution of the flow described by the Euler equations was initially developed by Deshaies et al. (1979) for relatively slow flames (Mach number $M_F = D/a_0 < 0.35$) and was extended by P. Cambray et al. (1979) for the case of rapid flames $(M_F \to \infty)$. This solution indicates that the flow generated by such deflagration can be divided into three regions:
-The burnt gas region bounded by the radius of the flame front R_F $(0 < R < R_F)$
- The fresh gas region bounded by the flame front and the spherical wave head of the range R_s in which the ambient gas is set in motion by the wave head propagating at the speed of sound in the ambient gas $(R_F < R < R_s = a_0 t)$. In this region, the following areas are defined:

- a thin layer near the piston $(R \approx R_F)$ where the flow is incompressible
- a central area where the hydrodynamic fields are acoustic
- a thin nonlinear zone (discontinuity) that indicates the transition between the flowing gas and the quiescent medium: the wave head in the range Rs. Its amplitude remains almost undetectable until the Mach number $M_P (M_P = u_P/a_0)$ of the piston is less than 0.35.

-The region of ambient gas at rest beyond the wave head $(R > a_0 t)$
The velocity field $u(R,t)$ and the pressure $\Delta P(R,t)$ are expressed as:
- Near the front ($R \sim R_F$), the flow is incompressible

$$\Delta P(R,t) = 2\rho_0 D^2 (1-\alpha)\left(\frac{R_F}{R}\right)\left[1-\frac{1-\alpha}{4}\left(\frac{R_F}{R}\right)^3\right]$$

$$u(R,t) = D(1-\alpha)\left(\frac{R_F}{R}\right)^2$$

- Far from the front ($R \gg R_F$), the flow is acoustic:

$$\Delta P(R,t) = 2\rho_0 D^2 (1-\alpha)\left(\frac{R_F}{R}\right)\left[1-\frac{R}{a_0 t}\right]$$

$$u(R,t) = D(1-\alpha)\left(\frac{R_F}{R}\right)^2\left[1-\left(\frac{R}{a_0 t}\right)^2\right]$$

The maximum overpressures observed in $R = R_F$ are defined as:

$\Delta P_{max} = 2\rho_0 D^2 (1-\alpha)\left(1-\frac{1-\alpha}{4}\right)$ in the incompressible area

$\Delta P_{max} = 2\rho_0 D^2 (1-\alpha)\left(1-\frac{D}{a_0}\right)$ in the acoustic zone

However, for large volumes of gas, the relationship between the speed of propagation D and the fundamental speed of the flame is corrected as follows:
$D = \alpha^{-1} V_F k$

where k is an empirical coefficient determined from experiments such that $1<k<2.5$. This factor reflects the observed increase in the effective area of the flame front relative to the perfectly spherical laminar front. Indeed, the flame front during propagation undergoes structural changes. At the beginning and for small radii, the front is laminar; a cellular structure then appears as the radius increases.

5.1.2. Explosions at variable speeds

Many experiments regarding gas explosions have demonstrated that the speed of the flame is often variable.

The explosion creates a flow similar to that produced by a semipermeable spherical piston, which moves at a speed of $u_P(t)$, and the instantaneous velocity of the piston is related to the instantaneous speed of the deflagration (Deshaies et al., 1981). In fact, according to the conservation of mass equation across the combustion wave, the piston speed is equal to:

$$u_P(t) = D(t)(1-\alpha) \text{ with } D(t) = \frac{dR_F}{dt}$$

Assuming that the flame propagates at a variable speed in an infinite medium with the propagation law $R_F(t)$, the integration of the conservation of mass and impulse equations allows for a calculation of the pressure $\Delta P(R, t)$.

The velocity field $u(R,t)$ and pressure $\Delta P(R,t)$ terms are expressed as follows: near the $R \sim R_F$ front (incompressible flow)

$$\Delta P(R,t) = \frac{\rho_0}{R}(1-\alpha)\left[2R_F(t)\left(\frac{dR_F(t)}{dt}\right)^2 + R_F^2(t)\left(\frac{d^2R_F(t)}{dt^2}\right) - \frac{1-\alpha}{2}\frac{R_F^4(t)}{R^3}\left(\frac{dR_F(t)}{dt}\right)^2\right]$$

far from the front ($R \gg R_F$) (acoustic area)

$$\Delta P(R,t) = \frac{\rho_0}{R}(1-\alpha)\left[2R_F(\tau)\left(\frac{dR_F(\tau)}{d\tau}\right)^2 + R_F^2(\tau)\left(\frac{d^2R_F(\tau)}{d\tau^2}\right)\right]$$

where $\tau = t - \frac{r}{a_0}$, and t is the time from the ignition.

These equations indicate that the pressure field depends on the flame speed and acceleration. According to Cleaver et al. (1996) the equation in the vicinity of the front can be applied for R near R_F, and, in the case of an explosion, can reach up to 250 $m.s^{-1}$ compared to 120 ms^{-1} in the case of explosions that travel at a constant speed.

5.2. Adaptation of the Sachs method to deflagrations

5.2.1. Dorofeev solution (1995)

An adequate description of the effects of a blast includes the flame speed. In this case, the Sachs method cannot be used without some modifications. However, an estimate for the peak overpressure and impulse boundary of the cloud can be obtained according to the flame speed in a quasi-acoustic approximation. The work of Khul et al. (1972), Strehlow (1975) and Desbordes et al. (1978), which was compiled by Dorofeev et al. (1995a,b), results in the following description of the blast wave parameters:

$$\overline{P^+} = \min\left(\overline{P_1}, \overline{P_2}\right) \qquad \overline{I^+} = \min\left(\overline{I_1}, \overline{I_2}\right)$$

$$\overline{P_1^+} = \frac{0.34}{\overline{R^{4/3}}} + \frac{0.062}{\overline{R^2}} + \frac{0.0033}{\overline{R^3}}$$

$$\overline{P_2^+} = \frac{V_F^2}{c_0^2}\frac{\alpha-1}{\alpha}\left(\frac{0.83}{\overline{R}} - \frac{0.14}{\overline{R^2}}\right)$$

$$\overline{I_1^+} = \frac{0.0353}{\overline{R^{0.968}}}$$

$$\overline{I_2^+} = \frac{V_F}{c_0}\frac{\alpha-1}{\alpha}(1-0.4\frac{V_F}{c_0}\frac{\alpha-1}{\alpha})\left(\frac{0.06}{\overline{R}} + \frac{0.06}{\overline{R^2}} - \frac{0.06}{\overline{R^3}}\right)$$

where:

$$\overline{R} = R\frac{P_0^{1/3}}{E^{1/3}} \quad \overline{P} = \frac{P}{P_0} \quad \overline{I} = \frac{I a_0}{E^{1/3} P_0^{1/3}}$$

Here, V_F is the apparent speed of the flame, a_0 is the velocity of sound in air at a pressure P_0, α is the expansion ratio, R is the distance from the center of explosion, E is the energy released by the chemical reaction and P and I are the overpressure and positive impulse of the blast wave measured in R, respectively.

The equations with subscript 2 are valid for flame speeds below 300 ms^{-1}. For higher flame speeds (up to 500 ms^{-1}) the parameters are given by $\overline{P}$ and $\overline{I}$. All of these equations are valid for $0.33 \leq \overline{R} \leq 3.77$ and flame speeds up to 500 ms^{-1}.

5.2.2. Dobashi solution (2008)

Dobashi (2008) proposed a theoretical expression of the pressure wave resulting from an explosion, which was observed at a given distance R from the center of the explosion and based on acoustic wave theory. This equation was then modified to account for hydrodynamic instabilities and a thermo-diffusive flame. Validation of this expression was obtained from a comparison with large-scale tests.

The maximum pressure of a blast wave resulting from an explosion is then expressed by:

$$P_{max} = \frac{21}{4}\frac{\rho}{R} c_g^{4/3} R_0^{5/3} k_T^{-2/3} \alpha^{5/3} (\alpha - 1) V_F^{8/3}$$

where ρ is the density, c_g is a constant equal to 0.0023, R_0 is the initial radius of the flammable mixture, k_T is the thermal diffusivity of the ambient gas, α is the ratio of volume expansion and V_F is the burning rate.

This equation was derived under the assumption that the maximum pressure occurs if all of the flammable mixture is burned ($R = \alpha^{1/3} R_0$). From this equation, the peak overpressure is proportional to $V_F^{8/3}$.

6. Blast waves resulting from an explosion in an obstructed space

The flame propagation is strongly influenced by its environment. Consequently, if the flame

propagates in turbulent flow in an environment that is congested or obstructed, then the flame front wrinkles due to large eddies and turbulent transport and so the flame front area increases and changes the flow upstream, which can lead to acceleration and a transition to detonation. Therefore, an evaluation of the external mechanical effects resulting from an explosion in this context requires the appropriate methods. This is the subject of methods known as *multi-energy methods* and the analytical relationship from Dorofeev (2005)

6.1. Dorofeev model (2005)

The methodology presented in a previous work (Dorofeev, 1995) (section 5.2.1) has been applied to the propagation of flame in obstructed area. The expression of pressure and impulse are not change. The flame speed is reformulated. The flame speed increases due to the increase of the flame area in an obstacle and to the increase of the turbulent mixing burning rate flame propagation. Hence, Dorofeev (2005) gives a description of the flame speed V_F as a function of distance R in an area with obstacles, the integral length of turbulence L_T, the laminar burning velocity S_L, the laminar flame thickness δ, the expansion ratio α, the distance between obstacle x and the characteristic size of obstacles y.

$$V_F = a^2 b\alpha(\alpha-1)S_L\left(1+\frac{4}{3}\frac{\alpha y}{x}\frac{R^\beta}{(\alpha x)^\beta}\right)^2\left(\frac{L_T}{\delta}\right)^{1/3}$$

with a, b and β are parameters determined by experiments. This model was validated for unconfined hydrogen explosion with different levels of congestion.

6.2. Multi-energy method: *basic concept*

Multi-energy methods are based on the concept that explosive combustion can only develop in a highly turbulent mixture or in obstructed areas of a cloud and/or if they are partially confined. An explosion is likely to generate high pressures if the flames reach a high velocity (several tens of m/s) or if the gases are confined by walls.

Thus, the multi-energy concept differs from conventional methods in that a gas explosion can no longer be considered as an entity but instead as a set of sub-explosions or elementary explosions, which corresponds to the number of areas in which the flammable clouds burn under highly turbulent conditions.

Consequently, the concept of the multi-energy method is based on:

1. the number of explosions
2. the characterization of each explosion in terms of: i) the density of obstacles; ii) the degree of containment; iii) the form and dimensions of the flammable cloud; iv) the reactivity of the fuel; v) the energy and position of the source of ignition; and vi) the turbulence in the reactive region.

There are two types of multi-energy methods: TNO (Netherlands Organization for Applied Scientific Research) and Baker and Strehlow - Baker and Strehlow-Tang (BS-BST), which are presented below.

6.3. TNO multi-energy method

The TNO method (CPR 1997, Van den Berg, 1985) uses force as the major index and considers the degree of confinement and ignition energy. The severity of each elementary explosion can be characterized using an index of blast strength between 1 and 10. An index of 10 corresponds to a detonation, and the intermediate indices correspond to various flame speeds, which increase with

an increase in the index number. Some recommendations have been given by different authors regarding the choice of the indices.
In the Yellow Book (CPR 1997), the index is chosen based on the following recommendations: 10 for all index volumes corresponding to areas congested with obstacles if the flammable cloud is characterized by a large turbulent agitation (gas discharge) and an index of 1 for all volumes that do not correspond to congested areas.
Kinsella (1993) proposed indices that account for the ignition energy, the degree of congestion and the degree of confinement (Table 11). The reactivity of the fuel is not explicitly taken into account.

Table 11 TNO method multi-energy type - Matrix Kinsella (1993)

Ignition energy		Level of obstruction			Degree of confinement		Blast strength
Weak	Strong	Weak	Strong	Not Established	Established	Not Established	
	X	x			X		7 – 10
	X	x				x	7 – 10
X		x			X		5 – 7
	X		x		X		5 – 7
	X		x			x	4 – 6
	X			X	X		4 - 6
X		x				x	4 – 5
	X			X		x	4 – 5
X			x		X		3 – 5
X			x			x	2 – 3
X				X	X		1 – 2
X				X		x	1

This index results from a characterization of the pressure and the duration of the positive phase of the pressure wave (Figs. 5-6).

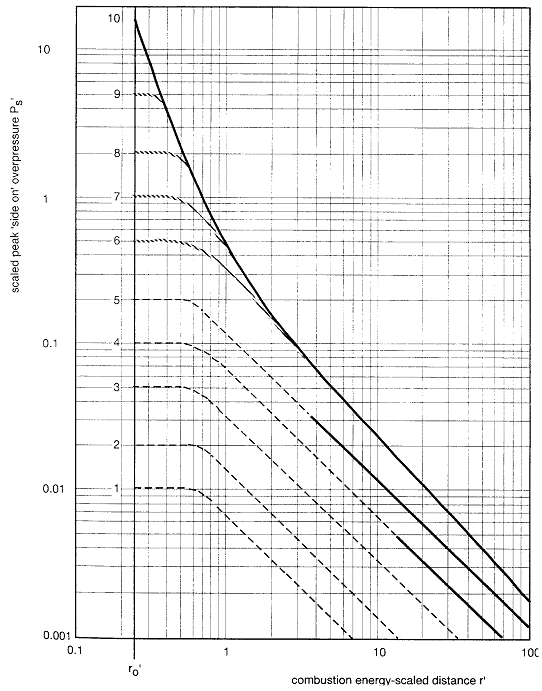

Fig. 5. Reduced pressure - TNO type multi-energy method (CPR, 1997)

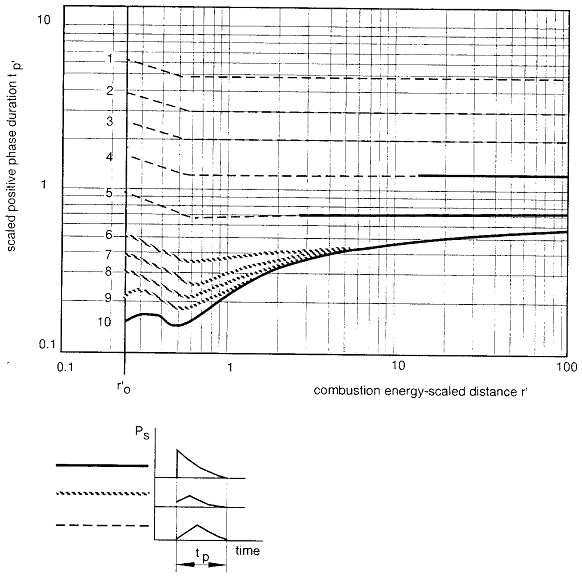

Fig. 6. Reduced positive phase duration - TNO type multi-energy method (CPR, 1997)

The TNO curves indicate the overpressure and positive phase duration with respect to the distance to the center of the explosion.

$$\bar{P} = \frac{P - P_0}{P_0} \qquad \bar{R} = \frac{R}{\left(\frac{E}{P_0}\right)^{1/3}} \qquad \bar{t}_+ = \frac{t_+ \; a_0}{\left(\frac{E}{P_0}\right)^{1/3}}$$

where $\bar{P}$ is the reduced pressure (dimensionless), $\bar{t}_+$ is the reduced duration of the positive phase (dimensionless), $\bar{R}$ is the reduced distance (dimensionless), P_0 is the atmospheric pressure (Pa), a_0 is the velocity of sound under ambient conditions (m/s), P is the absolute peak pressure (Pa), R is the distance from the center of explosion (m), E is the total energy released from the center (J) and t_+ is the positive phase duration (s).

The curves (Figs. 5 - 6) with indices of 6, 7, 8, 9 and 10 converge to $\bar{R} = 2$ and 10 for the pressure and duration, respectively.

6.4. The BS-BST type multi-energy method

The BS-BST type multi-energy method is based on the Mach number of the flame (flame velocity/sound velocity) and the reactivity of the fuel. Two separate cases are considered: 1) the Strehlow and Baker method (BS) (Baker et al., 1996), in which the Mach number (M_w) is the Lagragian Mach number; 2) the Baker, Strehlow and Tang method (BST) (Tang et al., 1999) and in which the Mach number M_f is Eulerian.

For the BS-BST type multi-energy method, the parameter that is used to obtain the properties of the blast wave is the flame speed. Regarding the estimation of flame speed, two matrices have been proposed. The matrix from Baker et al. (1996) is applicable to the standard BS method, and the matrix from Pierorazio et al. (2004) is validated for the BST type method. The Baker et al. matrix (1996) is based on a compilation of experimental results for flame speed. This compilation presents a correlation between the reactivity of the fuel, the density of obstacles and the confinement.

Table 12
Baker et al. matrix (1996)

1D Extension (flame in a tube)			
Reactivity	Obstacle Density		
	H	M	L
H	M_w = 5.2	M_w = 5,2	M_w = 5,2
M	M_w = 2.265	M_w = 1.765	M_w = 1.029
L	M_w = 2.265	M_w = 1.029	M_w = 0.294
2D Extension (cylindrical flame front)			
	Obstacle Density		
	H	M	L
H	M_w =1.765	M_w = 1.029	M_w = 0.588
M	M_w = 1.235	M_w = 0.662	M_w = 0.118
L	M_w = 0.662	M_w = 0.471	M_w = 0.079
3D Extension 3D (spherical or hemispherical flame)			
	Obstacle Density		
	H	M	L
H	M_w = 0.588	M_w = 0.153	M_w = 0.071
M	M_w = 0.206	M_w = 0.100	M_w = 0.037
L	M_w = 0.147	M_w = 0.100	M_w = 0.037

The influence of barriers is determined by experiments in which various obstacles are studied (cylinders, rectangles). The parameters studied are the blockage volume ratio (BVR), which is the volume occupied by obstacles over the total volume of space that contains the obstacles, and the pitch, which is the space between two consecutive barriers.
The classification with respect to the density of obstacles is based on the BVR as follows: for L, VBR < 10%; for M, 10% < VBR < 40%; and for H, VBR > 40%. The classification compared to the fuel reactivity is such that H is characteristic of hydrogen, acetylene, ethylene oxide and propylene oxide, M is characteristic of other compounds and L is characteristic of methane and carbon monoxide.
In this matrix, the flame speed is selected by using three dominant parameters for the propagation of a flame: the flame speed, the reaction mixture and the density of obstacles present in the course of the flame. However, the case of a 1D confinement is very uncommon in industry.
The Pierorazio et al. matrix (2004) is based on the results of medium-scale experiments. The blocked regions were composed of modular cubical sections. The size of each cube was 1.8 x 1.8 x 1.8 m. The obstacles were tubes with a circular cross section. To achieve different levels of obstruction, the number of tubes was varied: 16 for low congestion, 49 for average congestion and 65 for high congestion. The results include overpressures and flame speeds. The mixtures used in the tests were a stoichiometric mixture of methane and air in the case of low obstruction, a stoichiometric mixture of propane and air in an average level of congestion and a stoichiometric mixture of ethylene and air in the case of a high level of obstruction.

Table 13
Pierorazio et al. matrix (2004)

Confinement	Reactivity	Congestion		
		L	M	H
2D	H	$M_f = 0.59$	DDT	DDT
	M	$M_f = 0.47$	$M_f = 0.66$	$M_f = 1.6$
	L	$M_f = 0.079$	$M_f = 0.47$	0.66
2.5D	H	$M_f = 0.47$	DDT	DDT
	M	$M_f = 0.29$	$M_f = 0.55$	$M_f = 1.0$
	L	$M_f = 0.053$	$M_f = 0.35$	$M_f = 0.50$
3D	H	$M_f = 0.36$	DDT	DDT
	M	$M_f = 0.11$	$M_f = 0.44$	$M_f = 0.50$
	L	$M_f = 0.026$	$M_f = 0.23$	$M_f = 0.34$

DDT:Deflagration-to-Detonation Transition

The classification for reactivity and congestion is identical to the Baker et al. (1996) matrix
The following two matrices show that if the Lagrangian Mach number (M_w) and the associated maximum overpressure is known, then the Eulerian Mach number (M_f) can be calculated by using the following equation:

$$\frac{P_{max} - P_0}{P_0} = 2.4 \frac{Mf^2}{1 + M_f}$$

where P_{max} is the maximum pressure, P_0 is the atmospheric pressure and M_f is the Eulerian Mach number (flame speed/speed of sound).

An estimation of the flame speed allows the properties of the reduced blast wave to be determined by using the following charts (Figs. 7 - 10), which show different curves for the TNO type multi-energy method. The evolution of the overpressure and impulse as a function of distance is shown as a curve, and the flame speed separates the different groups of curves. The curves from the Baker-Strehlow method (BS and BST) allow the positive pressure (Figs. 7 - 8) and impulse (Fig. 9-10) to be determined as a function of the distance. The reduced impulse is defined by $\bar{I} = \frac{I\, a_0}{E^{1/3}\, P_0^{2/3}}$, where "I" is the specific impulse (Pa.s).

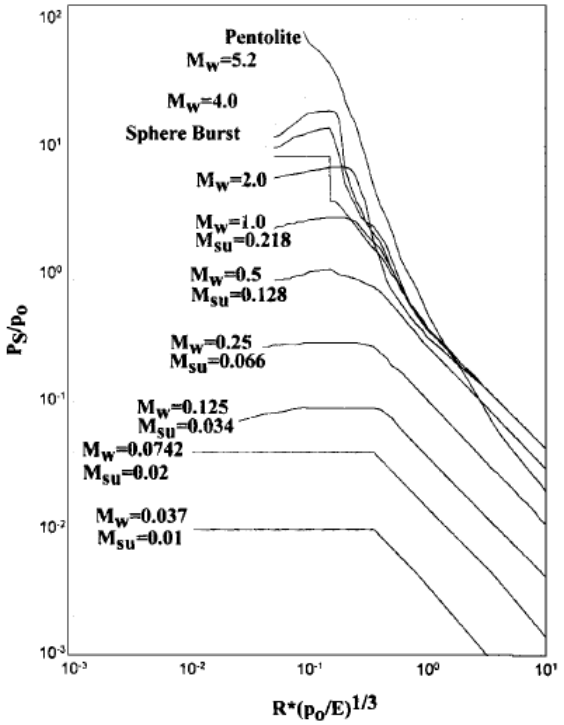

Fig. 7. BS Method - Reduced positive pressure as a function of reduced distance for different Lagrangian Mach number (Baker et al., 1996).

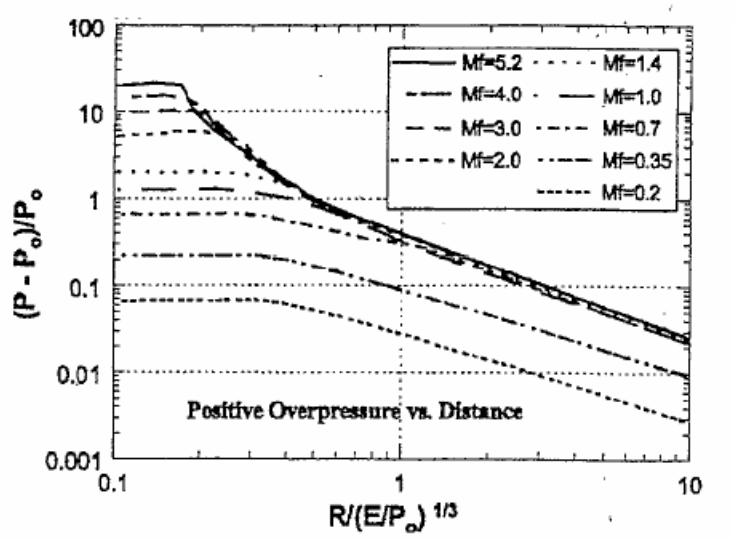

Fig. 8. BST method – Reduced positive pressure as a function of reduced distance for different Eulerian Mach number (Tang et al., 1999)

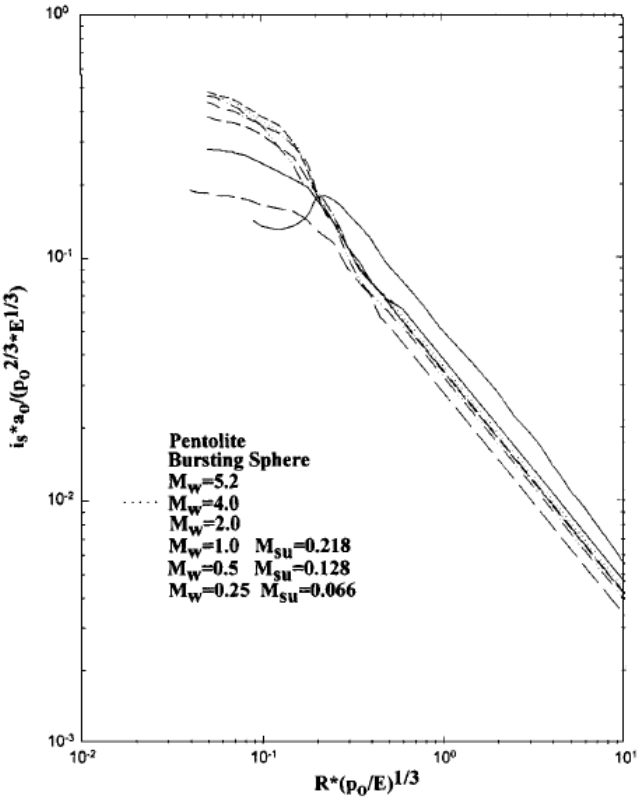

Fig. 10. Reduced positive impulse as a function of reduced distance for different Lagrangian Mach number (Baker et al., 1996).

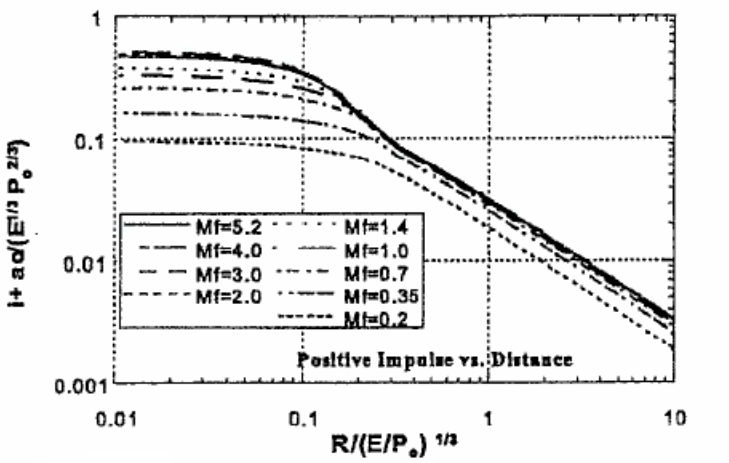

Fig. 10. Reduced positive impulse as a function of reduced distance for different Eulerian Mach number (Tang et al., 1999)

7. Conclusions

In contrast to the expensive computational time and capacity that is required for methods involving computational fluid dynamics, analytical methods for evaluating characteristic parameters of the blast wave from an explosion are useful, despite their limitations. This article provides an overview of these models and highlights their limitations. The validated methods have the advantage of rapid implementation, which is useful for a preliminary, on-site study in an emergency situation.

The TNT equivalent method assumes both that the entire gas mixture is involved in the explosion and that the explosion propagates in an idealized manner, but this method does not consider the presence of obstacles. The TNO type multi-energy method as well as the BS and BST methods account for the contribution of areas of congestion for the generation of blast waves.

There is some difficulty in applying these three methods. In the case of the TNT equivalent method, it is necessary to specify a yield for the explosion, and the result varies depending on the chosen value.

The two major differences between the multi-energy methods (BS, BSTinvolve the identification of the reduced properties (index of severity, speed of flame) of blast waves. In addition, the curves resulting from the TNO type multi-energy method give the reduced pressure and the duration of the positive phase. For the BST curves, the reduced properties that are obtained are the reduced pressure and reduced impulse. However, the overall trend of the curves remained the same with a plateau in the near field (zone of exhaust gases) and damping curves in the far field (acoustic area).

For the multi-energy TNO method, the choice of index is at the discretion of the user and is not very guided. Regarding the BST methods, the choice of Mach number is more important. Indeed, the waves of the BV and the levels of containment are defined, and this choice leads to a more objective result than in the case of the TNO multi-energy method.

It is difficult to compare the results of these three methods because they are based on different assumptions. Nevertheless, a comparison was conducted by Quest (1999) by converting the TNT model based on dimensionless quantities identical into those used in the multi-energy models.

The conversion was performed by assuming a heat of combustion of 45 $MJ.kg^{-1}$ for all hydrocarbons. A comparison of the pressures was then conducted by considering the TNT model with a yield of 10%, the TNO multi-energy type model with an index of blast loading of 5 and the BS multi-energy model type with a Lagrangian Mach number of 0.25. As expected, the differences are very important for both near-field and far-field results.

References

Akhavan J. The chemistry of explosive. Royal Society of Chemistry (Great Britain), 2nd ed.; 2004.

ASTM - The ASTM computer program for chemical thermodynamic and energy release evaluation CHETAH 7.3, August 2001.

Baker WE. Explosions in Air. Austin, University of Texas Press, 1973.

Baker QA, Tang MJ, Scheier EA, Silva GJ. Vapor Cloud Explosion Analysis, Process Safety Progress 1996; 15(2):106-109.

Behrens K, Schneider H. Ausbreitungsfunktionen sphärischer Luftstosswellen für den Fall detonierender Äthylen-Luft-Gemische. Fraunhofer ICT; December 1975.

Brossard J, Leyer JC, Desbordes D, Saint-Cloud JP, Hendrickx S, Garnier JL, Lannoy A, Perrot JL. Air blast from unconfined gaseous detonations. Proc. 9th Int. on Col. On Dynamics and Reactive Systems, Poitiers, France, Progress in Astro. And Aero. 1985;94:556-566.

Brossard J, Bailly P, Desrosier C, Renard J. Overpressures imposed by a blast wave. Progress in Astronautics and Aeronautics 1988; 114:329-400.

Cambray P, Deshaies B, Clavin P. Solution des équations d'Euler associées à l'expansion d'une sphère à vitesse constante. J. de Physique 1979; sup. 11, 40:19-29.

Cleaver RP, Robinson CG. An analysis of the mechanisms of overpressure generation in vapour cloud explosions, J. of Hazardous Materials 1996; 45:27-44.

CPR, Committee for the Prevention of disaster. Yellow Book, Methods for the calculation of physical effects, Part 2, CPR 14E, Chap. 5, 3rd edition, 1997.

Cooper PW. Explosives Engineering, Wiley-VCH, 1996.

Deshaies B, Clavin P. Effets dynamiques engendrés par une flamme sphérique à vitesse constante. J.de Mécanique 1979; 18(2):213-223.

Dobashi R. Study on consequence analyses of blast wave generated by gaseous deflagrations. 7th Int. Symp. On Hazards, Prevention, and Mitigation of Industrial Explosions, St Petersburgh, Russia, July 7-11, 2008;322-329.

Deshaies B, Leyer JC. Flow Field induced by unconfined Spherical accelerating Flames. Comb. and Flame 1981;40:2-13.

Desbordes D, Manson N, Brossard J. Explosion dans l'air de charges sphériques non confinées de mélanges réactifs gazeux, Acta Astronautica, Pergamon Press 1978 ; 5 :1009-1026.

Dewey JM. The TNT equivalence of an optimum propane-oxygen mixture. J. Phys. D.: Appl. Phys. 2005; 4245-425.

Dorofeev SB. Blast effects of confined and unconfined explosions. Proc. of the 20th Int. Symp. on Shock waves, 1, 77-86, Pasadena, California, USA, ISBN 981-02-2957-7; 1995, a.

Dorofeev S.B., Sidorov V.P., Dvoinishnikov A.E. Blast parameters from unconfined gaseous detonations. Proc. of the 20th Int. Symp. On Shock waves, 1, 673-678, Pasadena, California, USA, ISBN 981-02-2957-7; 1995, b.

Dorofeev S.B. Evaluation of safety distances related to unconfined hydrogen explosions, Int. J.of Hydrogen Energy 2007; 32:2118 – 2124.

Esparza ED. Blast measurements and equivalency for spherical charges at small scaled distances. Int. Journal Impact Eng. 1986; 4(1):23-40.

Filler WS. Post-detonation and thermal studies of solid high explosives in a closed chamber. Comb. of explosives and solid propellants 1956; 648-657.

Gelfand B. Translation from Russian to English "Blast effects caused by explosions" authorized by B.Gelfand and M. Silnikov. United States Army, European Research Office of the U.S. Army. London, England. Contract Number N62558-04-M-0004, April 2004.

Jeremie R, Bajie Z. An approach to determining the TNT equivalent of high explosives. Scientific. Technical Review 2006; I.VI.(1):58-62.

Health &Safety Executive. The effects of explosions in the process industries. Loss Prevention Bulletin 1986;68:37-47

Kinney GF, Graham KJ. Explosives shocks in air, Second edition, Springer-Verlag 1985.

Kinsella K.G. A rapid assessment methodology for the prediction of vapour cloud explosions. Research report n° 357, Technical Research Centre of Finland,1993.

Kleine H, Dewey JM, Oashi K, Mizukai T, Takayama K. Studies of the TNT equivalence of

silver azide charges, J. Shock Waves 2003; 13:123-138.

Kogarko SM, Adushkin VV, Lyamin AG. An investigation of spherical detonations of gas mixtures. Int. Chem. Eng. 1966; 6:93-401.

Kuhl AL, Kamel MM, Oppenheim AK. On flame generated self-similar blast wave, 14th Symposium Int. on Combustion, The Combustion Institute, The Pennsylvania State University, USA, 1972; Issue 11201-1214.

Lannoy A. Analyse des explosions air-hydrocarbure en milieu libre : Etudes déterministe et probabiliste du scénario d'accident. Prévision des effets de suppression. Bulletin Direct. Etudes et Recherches EDF. A4,1984.

Meyer R. - Explosives. Third Edition, VCH Verlagsgesellschaft mbH, Weinheim, Germany, 1987.

NASA Lewis Research Center http://www.me.berkeley.edu/gri_mech/data/thermo_table.html

Ohashi K, Kleine H, Takayama K. Characteristics of blast waves generated by milligram charges. Proc. 23rd Int. Symp. on Shock waves, Fort Worth, USA, Lu F. (ed.) 2002; 187-193.

Omang M, Christensen SO, Borve S, Trulsen J. Height of burst explosions: a comparative sudy of numerical and experimental results. J. Shock Waves 2009; DOI 10.1007/s00193-009-0196-8.

Pförtner H. Gas cloud explosions and resulting blast effects. Nuclear Engineering and Design 1977; 41:59-67.

Pierorazio JA, Thomas JK, Baker QA, Ketchum DE. An Update to the Baker-Strelhow-Tang Vapor Cloud Explosion Prediction Methodology Flame Speed Table, Process Safety Progress 2005,24(1):59-65.

Quest Consultants Inc. A comparison of vapor cloud explosion models, Part II. The Quest Quarterly 1999; 4,Issue 2.

Scilly NF. Measurement of the explosive performance of high explosives. J.l of Loss Prevention in the Process Industries 1995; 8(5):265-273.

Sochet I, Schneider H. Blast Wave Characteristics and Equivalency. 7th International Symposium on Hazards, Prevention, and Mitigation of Industrial Explosions, St Petersburg, Russia, 7-11 July 2008

Strehlow RA. Blast waves generated by constant velocity flames: a simplified approach, Comb. and Flame 1975; 24:257-261.

Tang MJ, Baker QA. A New Set of Blast Curves from Vapor Cloud Explosion, Process Safety Progress, 1999; 18(3):235-240.

TM5.1300. Departments of the Army, the Navy and the Air Force. Structures to resist the effects of accidental explosions. Technical Manual, NAFVAC-P397 / AFM88; 1969.

Tongchang Y, Menchao Y, Jianling W. Determination of heats of detonation and influence of components of composite explosives on heats of detonation of high explosives. J. of Thermal Analysis 1995; 44:1347-1356.

Trélat S. Impact de fortes explosions sur les bâtiments représentatifs d'une installation industrielle. Thèse de Doctorat de l'Université d'Orléans, France, 07 décembre 2006.

Trélat S, Sochet I, Autrusson B, Loiseau O, Cheval K. Strong explosion near a parallelepipedic structure. J. Shock Waves 2007 ;16(4-5):349-357.

Van den Berg AC. The multi-energy method: a framework for vapor cloud explosion blast prediction, J of Hazardous Materials 1985; 12(1):1-10.